Budding of lipid bilayer vesicles and flat membranes

1992 J. Phys.: Condens. Matter 4 1647

(http://iopscience.iop.org/0953-8984/4/7/004)

J. Phys.: Condens. Matter 4 (1992) 1647–1657. Printed in the UK

Budding of lipid bilayer vesicles and flat membranes

W Wiese, W Harbich† and W Helfrich
Fachbereich Physik, Freie Universität Berlin, Arnimallee 14, 1000 Berlin 33, Federal Republic of Germany

Received 21 October 1991

Abstract. We reconsider vesicle budding, this time including (besides bilayer bending elasticity) the energy of monolayer stretching, i.e. area dilation of one monolayer and compression of the other. Monolayer stretching during a shape change of the vesicle affects the spontaneous curvature of the membrane but, if measured values of material parameters are inserted in the equations, it turns out to be a minor perturbation. We also treat the budding of infinitely extended flat membranes where the spontaneous curvature is strictly constant during the deformation. The calculated shapes are compared to photographed buds in very large phosphatidylcholine membranes.

1. Introduction

The shape transformations of fluid bilayer vesicles have recently been studied, both theoretically [1–6] and experimentally [3–7]. A problem of particular interest in this context is the formation of buds (i.e. daughter vesicles still connected to the mother), which has been considered in all of these studies. Possible causes of shape transformations are changes in vesicle volume, membrane spontaneous curvature, or the area difference between the monolayers which constitute the bilayer. In the previous shape calculations either the spontaneous curvature, c_0, or the area difference, ΔA, were assumed to be independent of the shape, although their changes may induce the transformation. The constraints do not affect the possible equilibrium shapes, but those which are unstable in one case can be stable in the other. In particular, depending on whether the spontaneous curvature model (shape-independent c_0) or area difference model (shape-independent ΔA) were adopted, the budding transition was predicted to be discontinuous or continuous, respectively.

A complete model, comprising the c_0 and ΔA models as limiting cases, has been proposed in rudimentary ways some years ago [8–10]. It permits both ΔA and c_0 to change in a shape transformation, the two being related by the area dilation of one monolayer and the corresponding area compression of the other monolayer which accompany the shape change. We will call it here the monolayer stretching model.

The experimental observations [3–7], mostly made with dimyristoyl phosphatidylcholine bilayers, seem to be in favour of the ΔA model as they showed budding to proceed via pear-like shapes which are unstable in the c_0 model. The situation is not

† Present address: Bundesanstalt für Materialprüfung, Abteilung 6.2, Unter den Eichen 87, 1000 Berlin 45, Federal Republic of Germany.

0953-8984/92/071647 + 11 $04.50

quite clear, however, as the last stage of the budding transition—the closing of the constriction between daughter and mother—occurred abruptly and displayed hysteresis [7]. Sometimes the whole transition was abrupt, leading from an irregular sphere directly to the final mother–daughter pair.

In the following, we will argue that, in the case of phosphatidylcholine bilayers and similar lipid membranes, the spontaneous curvature model should be closer to reality than the other limiting case. This makes it worthwhile to consider 'pure budding' (i.e. the formation of a bud in an infinitely extended flat membrane), for which the c_0 model is correct in any event. We will show that pure budding, which takes place at positive lateral tension, always requires an activation energy and can occur only if the ratio of spontaneous curvature to lateral tension is large enough. Finally, an experimental demonstration of almost pure budding will be compared to the theoretical results.

2. Monolayer stretching model

The two monolayers in a fluid bilayer are free to slide over each other. They have different areas in a curved bilayer (e.g. a closed vesicle membranes). The difference in area, $\Delta A = A_{out} - A_{in}$, between the outer and inner monolayers of a vesicle membrane is given by

$$\Delta A = a \oint (c_1 + c_2)\, \mathrm{d}A. \tag{1}$$

Here c_1 and c_2 are the principal curvatures of the membrane (counted positive if they are convex towards the outside) and the length a is the distance between the neutral surfaces of the monolayers. Obviously, ΔA can change in a deformation and the change $\Delta^2 A$ is the difference between ΔA after the deformation and ΔA before the deformation:

$$\Delta^2 A = a \left[\oint_{\text{after}} (c_1 + c_2)\, \mathrm{d}A - \oint_{\text{before}} (c_1 + c_2)\, \mathrm{d}A \right]. \tag{2}$$

Let us assume that the two monolayers are practically identical and that the amount of lipid in either is constant. The latter assumption is justified by the very long characteristic times (of the order of hours) of lipid exchange with the aqueous media and of lipid flip-flop between the monolayers [11]. Under these circumstances a positive $\Delta^2 A$ means a uniform dilation, by $\Delta^2 A/2$, of the outer monolayer and an equal compression of the inner one. The double effect results not in a lateral tension but an additional couple per unit length, $\Delta\tau$, along a cut through the bilayer. Evidently,

$$\Delta\tau = \tfrac{1}{2} a k_s (\Delta^2 A)/A \tag{3}$$

where k_s is the stretching modulus of the bilayer. A positive torque tends to produce positive curvature. The couple is linked with a change in the spontaneous curvature of the bilayer Δc_0 through

$$\Delta\tau = -k_c \Delta c_0 \tag{4}$$

k_c being the bilayer bending rigidity [12]. Combining (3) and (4) yields

$$\Delta c_0 = -\tfrac{1}{2}(a k_s / k_c)(\Delta^2 A)/A. \tag{5}$$

For an estimate, it is convenient to view the monolayers as elastic plates of lateral

compression modulus k_s/h where h is the thickness of the bilayer. Accordingly, the neutral surfaces are in the middle of each monolayer, which implies $a = h/2$. In this model, the bending rigidity of the bilayer is easily seen to derive from its stretching modulus through [8, 12–14]

$$k_c = \tfrac{1}{12} k_s a^2. \tag{6}$$

Insertion of (2) and (6) in (5) leads to

$$\Delta c_0 = -\frac{\alpha}{A}\left[\oint_{\text{after}} (c_1 + c_2)\, dA - \oint_{\text{before}} (c_1 + c_2)\, dA\right] \tag{7}$$

with $\alpha = 3$. The same value of the numerical factor

$$\alpha = a^2 k_s / 4k_c \tag{8}$$

is obtained if one substitutes $k_s = 200\ \text{mN m}^{-1}$ and $k_c = (2/3) \times 10^{-19}\ \text{J}$ [15], both of which may be regarded as typical, and assumes $a = 2\ \text{nm}$ (i.e. about half the bilayer thickness). We believe that the real value of α does not differ by more than a factor of two from $\alpha = 3$ for DMPC bilayers and similar electrically neutral phospholipid and glycolipid membranes.

The shape equation for axisymmetric equilibrium shapes has been the basis of all treatments of budding. It is obtained from the general variational *ansatz*

$$\delta\left[\oint \tfrac{1}{2} k_c (c_1 + c_2)^2\, dA - k_c c_0 \oint (c_1 + c_2)\, dA + \lambda A + \Delta p\, V\right] = 0 \tag{9}$$

where the first two terms in the bracket represent the bending elastic energy of the bilayer for constant c_0. The spontaneous curvature, c_0, the bilayer lateral tension, λ, and the pressure difference, $\Delta p = p_{\text{out}} - p_{\text{in}}$, across the vesicle membrane can each be a Lagrange multiplier ensuring constancy of ΔA, A, and V, respectively, or the intensive parameter of a suitable reservoir. The membrane area, A, and the vesicle volume, V, are always considered to be constant in vesicle shape transformations, so that λ and Δp are Lagrange multipliers. However, c_0 is a Lagrange multiplier in the ΔA model but may be viewed as a reservoir parameter in the c_0 model (see below). In the monolayer stretching model, we take c_0 to be the initial spontaneous curvature and add the energy of monolayer stretching

$$\tfrac{1}{2} k_c \frac{\alpha}{A}\left[\oint_{\text{after}} (c_1 + c_2)\, dA - \oint_{\text{before}} (c_1 + c_2)\, dA\right]^2 \tag{10}$$

in the bracket of (9). This changes the spontaneous curvature by Δc_0, but does not affect the character of the shape equations.

The initial spontaneous curvature, c_0, can be of chemical origin, being due, for example, to unequal aqueous media inside and outside the vesicle. However, it can also arise from an initial non-equilibrium distribution of the lipids (i.e. monolayer compression and dilation) on which the deformation of the vesicle superimposes an additional imbalance.

A cross section of the vesicle containing the axis of rotation may be described by $\psi = \psi(x)$, where x is the local distance from the axis of rotation and ψ is the angle made

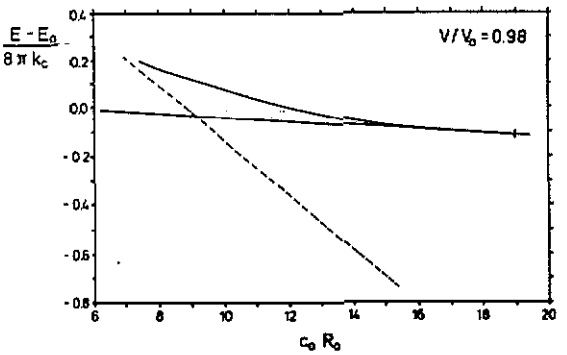

Figure 1. Reduced bending energies of equilibrium shapes as functions of reduced spontaneous curvature at constant $V/V_0 = 0.98$. The radius R_0, the volume $V_0 = (4\pi/3)R_0^3$, and bending energy E_0 refer to the sphere with $R_0 = (A/4\pi)^{1/2}$ where A is the constant membrane area. The spontaneous curvature is assumed to be independent of vesicle shape (c_0 model). The top curve represents unstable asymmetric shapes which, from right to left, are eggs, pears, and buds with an open constriction. It starts at $c_0R_0 \approx 19$ (not 16, as erroneously shown in [2]) from the curve of the symmetric elongated shapes which are nearly ellipsoidal. The symmetric shapes are locally stable for $c_0R_0 < 19$ and unstable for $c_0R_0 > 19$. The dashed curve represents the double sphere, i.e. a mother–daughter pair with infinitesimal constriction.

by the membrane and the equatorial planes of the vesicle. The principle curvatures, along the meridian and in the orthogonal direction, are then given by

$$c_m = \cos\psi \frac{d\psi}{dx} \qquad c_p = \frac{\sin\psi}{x}$$

Insertion in (9) leads to the shape equation

$$[\tfrac{1}{2}k_c(c_m + c_p)^2 - k_c(c_m + c_p - c_0 - \Delta c_0)c_m + \lambda]\, 2\pi x \sin\psi + \Delta p\, \pi x^2 - k_c \cos\psi\, d(c_m + c_p)/dx\, 2\pi x \cos\psi = 0 \qquad (11)$$

which can be rewritten in various ways for computer calculations.

Previous studies investigated how the budding of almost spherical vesicles proceeds while a shape-independent c_0 or ΔA is increased at fixed volume, or V is decreased at fixed c_0 or ΔA. Increasing ΔA at fixed volume, one may start from a prolate vesicle with equatorial reflection symmetry which, on becoming asymmetric, successively transforms into eggs, pears, and shapes with a constriction [3, 4]. The limiting shape of this continuous transition is a mother–daughter pair consisting of a large sphere and a smaller sphere connected by an ideally infinitesimal constriction.

The situation is very different if c_0 instead of ΔA is the shape-independent parameter whose change drives the transition. In this case the eggs, the pears, and part of the constricted shapes are unstable. In configurational space, they represent saddle points of the bending energy which are to be overcome on the way from near ellipsoids to highly constricted shapes and vice versa. This is illustrated by figure 1 which is taken from our previous publication [2]. The length $R_0 = (A/4\pi)^{1/2}$ is the radius of the sphere that can be formed from the fixed-membrane area A, and $V_0 = (4\pi/3)R_0^3$ is the volume of this sphere. The energies of the calculated ellipsoids and pass shapes are shown in figure 1 as functions of spontaneous curvature at constant vesicle volume, $V = 0.98V_0$. Also

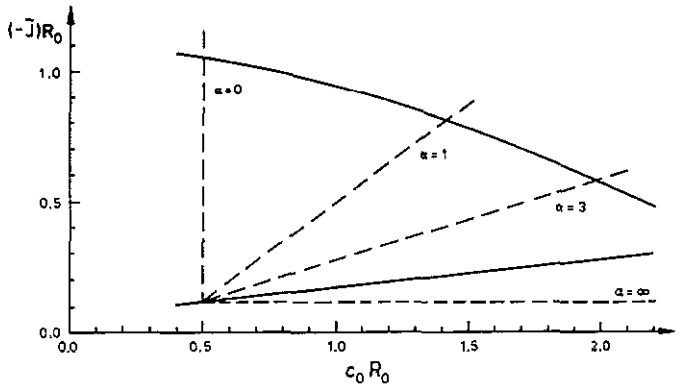

Figure 2. Arbitrary plot of the negative average curvature, J, against the actual spontaneous curvature, c_0 (or $c_0 + \Delta c_0$), for two branches of equilibrium shapes of the same vesicle (reduced values). The dashed lines of slopes $1/\alpha$ indicate how to find, for a particular shape on the lower branch, the related shape on the upper branch when the spontaneous curvature depends on shape. The two limiting cases, $\alpha = 0$ and $\alpha = \infty$, represent the c_0 and ΔA models, respectively.

shown are the energies of the mother–daughter pair with an infinitesimal constriction; the radius of the daughter is $0.1215\,R_0$. Their curve represents an upper limit for the energies of locally stable mother–daughter pairs. In complete calculations the energy curves of the unstable and locally stable asymmetric shapes emerge at a certain c_0 from a common starting point and the constriction of the locally stable shapes closes at some larger c_0 [3, 4]. Budding can take place where its activation energy becomes thermally accessible. As c_0 increases this will be the case only where the energy curve of the unstable shapes has come close to that of the ellipsoids. The topography of energy ridges and valleys in configurational space requires the ellipsoids to be unstable beyond this point.

In the monolayer stretching model, one has to take into account that the spontaneous curvature changes according to (7) as the initial ellipsoid deforms. In order to relate other equilibrium shapes to the initial one we can use the construction exemplified in figure 2. The two curves are arbitrary plots of the average curvature

$$\bar{J} = \frac{1}{A}\oint (c_1 + c_2)\,\mathrm{d}A \tag{12}$$

against the spontaneous curvature for two branches of equilibium shapes. Starting, for example, from the lower curve at $c_0 = 0.5R_0^{-1}$, we have to find the shape on the upper curve with the right spontaneous curvature. The spontaneous curvature of the new shape is $c_0 + \Delta c_0$ where Δc_0 has to obey

$$\Delta c_0 = -\alpha(\bar{J}_{\text{upper}} - \bar{J}_{\text{lower}}). \tag{13}$$

Any equilibrium shape satisfying this condition lies on the straight line, with slope $1/\alpha$, that also contains the starting point. The two limiting cases, $\alpha = 0$ and $\alpha = \infty$, represent the c_0 and ΔA models, respectively.

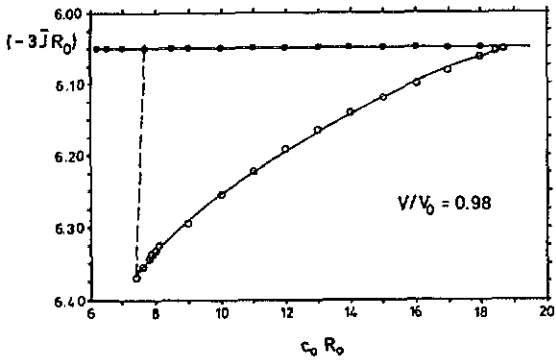

Figure 3. Plot of three times the negative average curvature against the actual spontaneous curvature (reduced values). The upper and lower curves represent symmetric shapes (near ellipsoids) and asymmetric shapes (pears etc), respectively. The dashed straight line of unity slope connects two related shapes.

The elastic energy difference between the equilibrium shapes related in this way may be expressed by

$$\Delta E = \tfrac{1}{2}k_c \oint_{\text{after}} (c_1 + c_2)^2 \, dA - \tfrac{1}{2}k_c \oint_{\text{before}} (c_1 + c_2)^2 \, dA - k_c c_0 \oint_{\text{after}} (c_1 + c_2) \, dA + k_c c_0 \oint_{\text{before}} (c_1 + c_2) \, dA + \tfrac{1}{2}k_c \frac{\alpha}{A} \left[\oint_{\text{after}} (c_1 + c_2) \, dA - \oint_{\text{before}} (c_1 + c_2) \, dA \right]^2 \tag{14}$$

where c_0 is the spontaneous curvature before the shape change and the last term is the energy of monolayer compression and dilation. For a proof of (14), one may imagine the compression and dilation to be accomplished after the membrane took its new configuration in contact with monolayer reservoirs that kept its spontaneous curvature constant.

To deal with budding, we assume $\alpha = 3$ and plot in figure 3 the quantity $-3\bar{J}R_0$ against c_0R_0 for the ellipsoids (upper curve) and the asymmetric shapes (pears etc, lower curve) of figure 1. As the scales on the two axes are so different, straight lines of slope unity relating shapes to each other are rather steep in this figure. We associated asymmetric shapes to the ellipsoids, which are regarded as the initial shapes, and calculated the energy difference (14) as a function of c_0. Similarly, we determined $\Delta c_0 R_0$ and the energy of the (immutable) mother–daughter pair with an infinitesimal constriction as functions of the spontaneous curvature of the initial ellipsoid. The integral $\bar{J}$ was taken here simply over the two spheres as there is no contribution to it from the infinitesimal constriction. The decrease of spontaneous curvature due to monolayer stretching and compression is stronger for the double sphere than for the more weakly deformed asymmetric shapes. We do not show the two new energy curves as they hardly differ from the corresponding curves of figure 1. The reduced energies of the double sphere, as defined in figure 1, are lifted by 0.033 while those of the unstable asymmetric shape are maximally raised by less than half this number. Obviously, monolayer stretching increases the barrier to budding, but it makes so little difference that the c_0 model may be regarded as a good approximation.

Figure 3 indicates that unrealistically large values of α (60 instead of 3) would be needed to approach the other limiting case, i.e. the ΔA model. Simple estimates suggest

that changes of the spontaneous curvature due to monolayer stretching should not alter the character of budding, including the extreme case of a daughter as large as the mother.

3. Pure budding

The budding of vesicles takes place on a curved membrane and may be outwards, as just considered, or inwards. The difference between the two directions will become insignificant if the mother is much larger than the daughter vesicle. Budding on an infinitely extended flat membrane (to be called 'pure budding') is equal in both directions. The spontaneous curvature model must be exactly valid in this case. Since α is so small ($\alpha \approx 3$), pure budding should still be a good approximation in many practical situations where the membrane area is finite.

The membrane configurations of pure budding are determined by two lengths, as may be seen from (11). They are the deflection length

$$\xi = (k_c/\lambda)^{1/2} \tag{15}$$

which characterizes the decay of a local perturbation of planarity and the curvature length

$$\zeta = 1/c_0 \tag{16}$$

which is the inverse of the spontaneous curvature. The shape, apart from size, depends only on the ratio of the two lengths or, if we disregard the direction of budding, on $(\zeta/\xi)^2 = \lambda/(k_c c_0^2)$. Either length can therefore be used to describe the size of the shape. Figures 4 and 5 show three equilibrium configurations of pure budding. As in the case of vesicles, the length R_0 is related through $4\pi R_0^2 = A$ to the surface area of the shape, as far as it is computed. New boundary conditions are required to deal with a 'vesicle' that is open on one side, so that its calculated contour ends at some $x = x_0$. Introducing the displacement of the membrane, $u = u(x)$, from the plane of the flat membrane, we assumed for $x \geqslant x_0$

$$u(x) = u_0 \, \mathrm{e}^{-(x-x_0)/\xi} \qquad \psi(x) = -\mathrm{d}u(x)/\mathrm{d}x \tag{17}$$

which should be good approximatins whenever $|\psi(x_0)| \ll 1$, so that c_p is much weaker than c_m at $x = x_0$. The energies of formation of these equilibrium shapes contain a term that accounts for the work of pulling in membrane area to form a bulge in the originally flat membrane. Inspection of the shape equation (11) shows the reduced energy to depend only on $(\zeta/\xi)^2$. The energy is plotted in figure 6 against $\lambda/(k_c c_0^2)$, or simply λ if c_0 is taken to be constant. The solid curve starting at the origin and ending where it merges with another piece of solid curve represents the unstable or pass shapes, i.e. wide bulges near the origin and buds with a narrow constriction at the end. The short full curve represents three locally stable shapes. The point on its left belongs to the shape of figure 4(*a*) which has the narrowest constriction of all the calculated shapes. There is little doubt that the line of locally stable solutions closely follows the dashed curve which gives the energy of spherical buds connected to a flat membrane by an infinitesimal constriction. The actual energies are slightly below this limiting curve before the constriction becomes infinitesimal at some unknown $\lambda/(k_c c_0^2)$. The same data plotted against $c_0(k_c/\lambda)^{1/2}$, or c_0 at constant λ, are displayed in figure 7.

The last two figures indicate that budding requires activation energies for all $\lambda > 0$. The barrier is very high at $\lambda/(k_c c_0^2) = 0.5$ where absolute stability changes from the bud

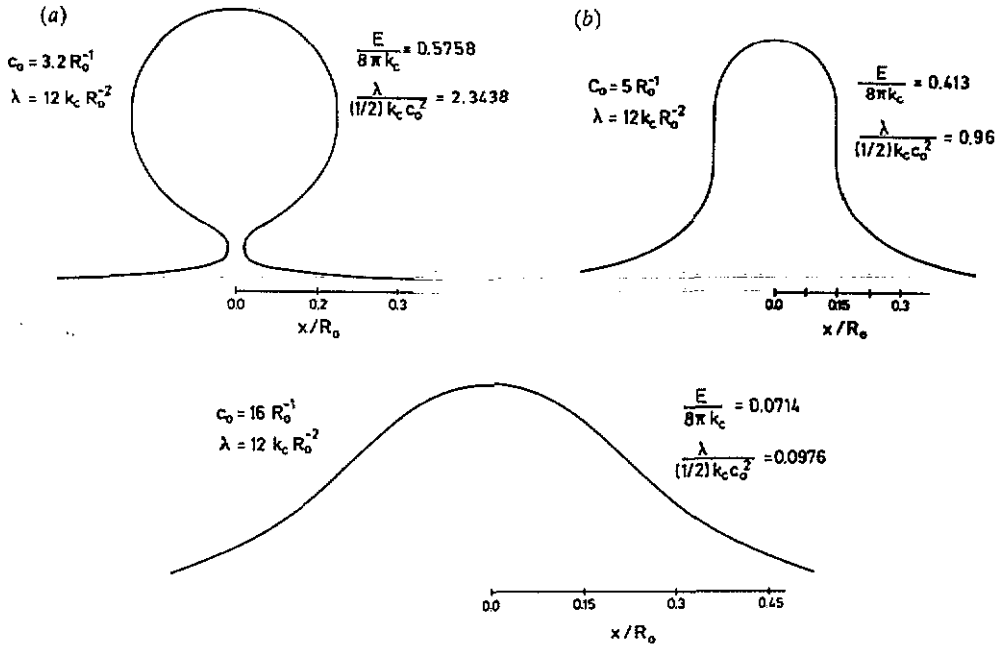

Figure 4. Cross sections containing the axis of rotation of three equilibrium shapes of pure budding: (*a*) for $c_0 = 3.2R_0^{-1}$, $\lambda = 12k_cR_0^{-2}$ (locally stable shape); (*b*) for $c_0 = 5R_0^{-1}$, $\lambda = 12k_cR_0^{-2}$ (unstable shape); and (*c*) for $c_0 = 16R_0^{-1}$, $\lambda = 12k_cR_0^{-2}$ (unstable shape). The scales are adapted to size.

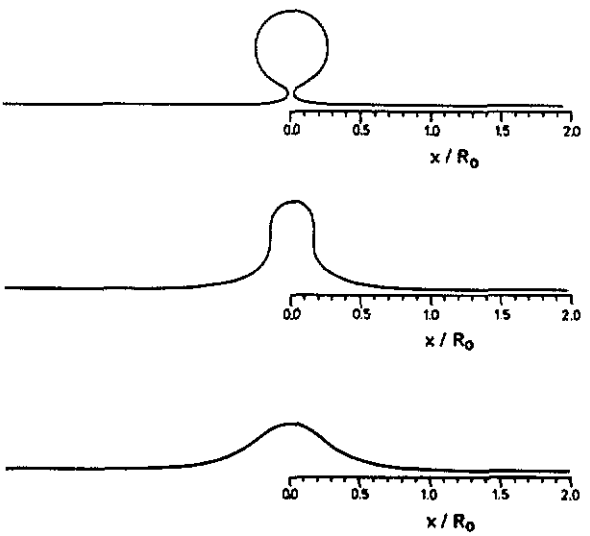

Figure 5. The three equilibrium shapes of figure 4 shown on equal scale and over the whole lengths of the calculated contours.

to the flat membrane. With $k_c = (2/3) \times 10^{-19}$ J one finds the changeover at $E = 7 \times 10^{-19}$ J $= 180\,k_BT$ for room temperature (k_B = Boltzmann's constant; T = temperature). Thermal activation within a reasonable period of time seems possible only if E is of the order of a few k_BT. A linear continuation of the calculated $E(\lambda)$ into the origin gives

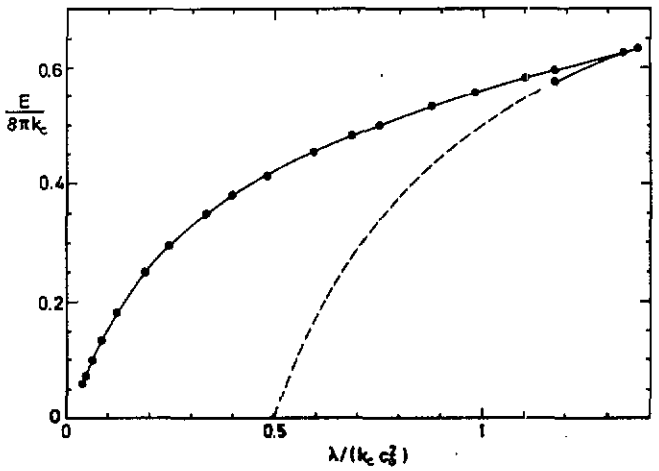

Figure 6. The reduced energies of the calculated equilibrium shapes of pure budding against $\lambda/(k_c c_0^2)$.

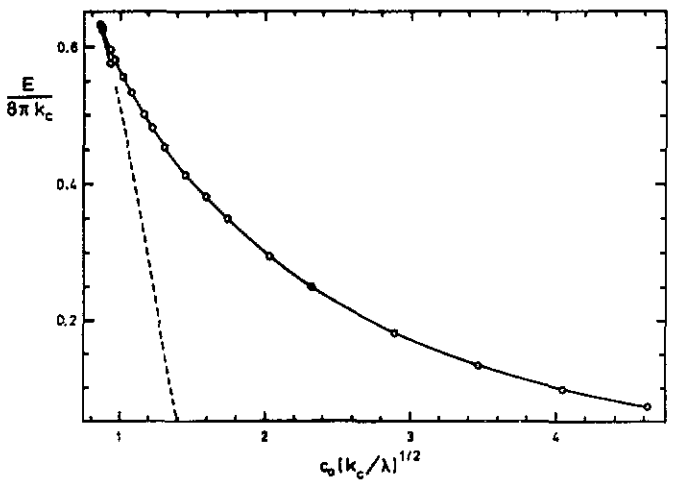

Figure 7. The reduced energies of the calculated equilibrium shapes versus $c_0(k_c/\lambda)^{1/2}$.

$\lambda/(k_c c_0^2) \approx 0.0015$ for $E = k_B T$. As a consequence, thermally activated pure budding may be expected to produce fully constricted shapes.

Some years ago we noticed that budding in very extended membranes can sometimes be achieved by mechanical activation, i.e. by touching the cover slide of the sample cell. The results of such an activation of egg yolk phosphatidylcholine bilayers are shown in figure 8 (shortly after the mechanical excitation) and figure 9 (about a minute later). The constrictions of the numerous buds are narrower at the later time, but they are still wider than may be expected on the basis of the locally stable equilibrium shapes shown in figures 4 and 5. (The ratio of the radii of constriction and equator is 0.078 for this shape. For the turning point of the energy curve at $\lambda/(k_c c_0^2) \approx 1.38$ we estimate the ratio to be 0.24, which is still less than the ratios read from figure 9.) The buds tend to disappear

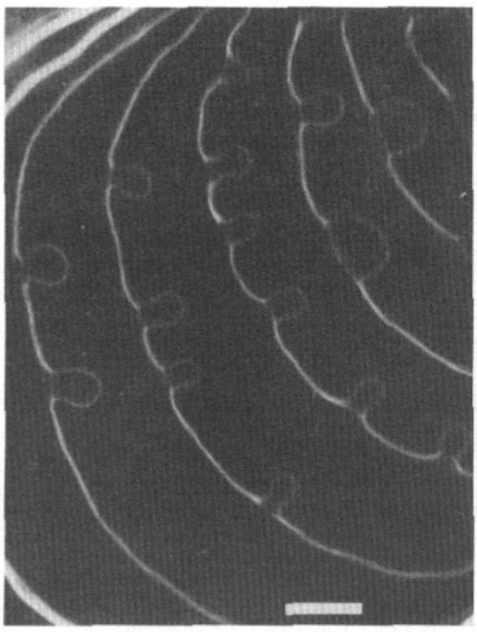

Figure 8. Buds forming in very extended egg yolk phosphatidylcholine membranes after mechanical shock, as seen in dark field microscopy. The bar represents 20 μm. Cell thickness was about 100 μm.

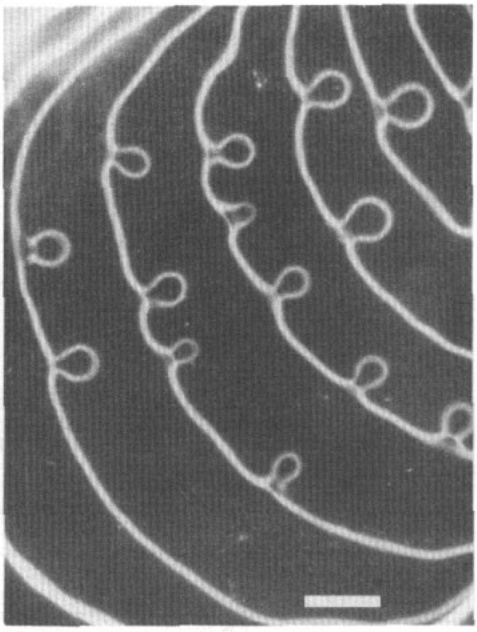

Figure 9. The same set of membranes as in figure 9 roughly a minute later. Note that two of the buds are about to disappear, the membrane returning to the flat state.

after a while, apparently by thermal activation, as may be seen by comparing figures 8 and 9. In the later photograph one bud has transformed into a gentle bulge and another is no longer constricted. On the other hand, further touches of the sample cell converted a few buds into separate vesicles.

The observations may be taken to suggest that the buds in all six membranes seen in the photographs are locally stable equilibrium states next to the point where the shapes turn unstable, i..e very near $\lambda/(k_c c_0^2) = 1/(\xi^2 c_0^2) = 1.3$. It is interesting to estimate the deflection length, $\xi = (k_c/\lambda)^{1/2}$, from figure 9 in two different ways. From the feet of the buds, which should approach the baseline exponentially (see above), we read $\xi = 2$–$3\ \mu$m. Comparing the radii, r, of the buds to the theoretical shape and its parameters, we find $r \approx 0.09R_0 \approx 0.72c_0^{-1}$ and thus $c_0 \approx 0.72/r$. The figure indicates $r \approx 4\ \mu$m which, with $\xi^2 = 1/(1.3c_0^2)$, leads to $\xi = 4.9\ \mu$m. The two estimates agree fairly well. However, the non-negligible difference of the two values for ξ, the constrictions that seem too wide, and especially the strange implication that $\lambda/(k_c c_0^2)$ should be in a narrow range of about 10 percent near the turning point of the energy curve for all the membranes, may raise some doubts about the agreement between theory and experiment.

4. Conclusion

We have shown that the budding of vesicles (made of common biological model membranes) should be an abrupt process, leading from an elongated shape to a mother–

daughter pair with a narrow or infinitesimal constriction. For this purpose, we used a model which comprises the two conflicting models of previous calculations as limiting cases and inserted known experimental numbers for the bilayer stretching modulus and the bending rigidity. The result leaves little or no room for a continuous budding transition through weakly asymmetric stable vesicle shapes such as eggs and pears. The fact that such transition states have been found experimentally appears very puzzling. Perhaps it has something to do with a superstructure of these membranes which was postulated for other reasons [16] and seems confirmed by electron microscopy [17, 18]. We may speculate that the superstructure, expected to develop in the absence of stress, resists strong deformations of the membranes. This could explain why vesicles prefer weakly asymmetric shapes over the final bud with its infinitesimal constriction. The superstructure may also intervene in the budding of very extended, practially flat membranes, as our photographed bud shapes do not fully agree with the theoretical predictions for pure budding. It may be worth mentioning, in a completely different context, that the theory of pure budding should also apply to the solubilization at interfaces, a process in which micelles are formed from a flat amphiphilic monolayer [19].

Acknowledgment

We are grateful to J Käs and E Sackmann for sending us their preprint. W Helfrich thanks J Käs for extensive discussions. When our work was completed a phase diagram of vesicle shapes covering the whole range between the c_0 and ΔA models was presented by U Seifert at the Workshop on Structure and Conformation of Amphiphilic Membranes, Jülich, Federal Republic of Germany, 16–18 September 1991. This work was supported by the Deutsche Forschungsgemeinschaft through SFB 312.

References

[1] Svetina S and Žekš B 1989 *Eur. Biophys. J.* **17** 101
[2] Wiese W and Helfrich W 1990 *J. Phys.: Condens. Matter* **2** SA 329
[3] Berndl K, Käs J, Lipowsky R, Sackmann E and Seifert U 1990 *Europhys. Lett.* **13** 659
[4] Seifert U, Berndl K and Lipowsky R 1991 *Phys. Rev.* A **44** 1182
[5] Miao L, Fourcade B, Rao M, Wortis M and Zia R K P 1991 *Phys. Rev.* A **43** 6843
[6] Wortis M, Seifert U, Berndl K, Fourcade B, Miao L, Rao M and Zin R K P 1991 *Workshop on Dynamical Phenomena at Interfaces, Surfaces and Membranes (Les Houches, 1991)* ed D Beysens, N Boccara and G Forgacs
[7] Käs J and Sackmann E 1991 *Biophys. J.* **60** 625
[8] Helfrich W 1974 *Z. Naturf.* c **29** 510
[9] Evans E A 1974 *Biophys. J.* **14** 923
[10] Svetina S, Ottova-Leitmannova A and Glaser R 1982 *J. Theor. Biology* **94** 13
[11] Wimley W C and Thompson T E 1991 *Biochemistry* **30** 1702
[12] See, for example, W Helfrich 1990 *Liquids at Interfaces (Les Houches XLVIII, 1988)* ed J Charvolin, J F Joanny and J Zinn-Justin (Amsterdam: Elsevier)
[13] Petrov A G and Bivas I 1984 *Prog. Surf. Sci.* **16** 389
[14] Evans E and Skalak R 1980 *Mechanics and Thermodynamics of Biomembranes* (Boca Raton, FL: Chemical Rubber Company)
[15] Evans E and Rawicz W 1990 *Phys. Rev. Lett.* **64** 2094
[16] See, for example, R M Servuss and W Helfrich 1989 *J. Phys. France* **50** 809
[17] Helfrich W and Klösgen B 1990 Dynamics and Patterns in Complex Fluids *Springer Proc. in Phys.* vol 52, ed A Onuki and K Kawasaki, and in the same proceedings as reference [6]
[18] Klösgen B and Helfrich W 1991 Preprint
[19] Nitsch W and Plucinski P 1990 *J. Colloid Interface Sci.* **136** 338